

# A UAV for Destructive Surveys of Mosquito Population

Mary Burbage, An Nguyen, Kyle Walker, Nhan Phung, Vinh Truong, Erik Van Aller, and Aaron T. Becker

**Abstract**—Mosquitoes are a vector for several deadly diseases which are responsible for killing millions of people each year. Popular methods to control mosquitoes such as insecticides are effective, but long-term effects of pesticides are of concern, particularly as mosquito species develop resistance over time. Traditional electrified screens (bug zappers) use UV light to attract pests but have a large by-catch of non-pest insects. This paper introduces techniques using electrified screens (bug zappers) mounted on unmanned vehicles to autonomously seek out and eliminate mosquitoes in their breeding grounds. Instrumentation on the bug zappers logs the GPS location, altitude, weather details, and time of each mosquito elimination. Mosquito control offices could use this information to analyze the insects' activities. The device can be mounted on a remote controlled or autonomous unmanned vehicle. If autonomous, the vehicle can use the data collected from the electrified net as feedback to improve the effectiveness of the motion plan. This paper examines design considerations, presents a working prototype system of a drone and instrumented bug zapper, and introduces a simulator for swarms of mosquitoes and a mosquito-eliminating drone.

## I. INTRODUCTION

Mosquito-borne diseases kill millions of humans each year [1]. Popular methods to control mosquitoes such as insecticides are effective, but they have the potential to introduce long-term environmental damage and mosquitoes have demonstrated the ability to become resistant to pesticides [2]. Traditional electrified screens (bug zappers) use UV light to attract pests but have a large bycatch of non-pest insects [3]. This paper introduces techniques using bug zappers mounted on unmanned vehicles to autonomously seek out and eliminate mosquitoes in their breeding grounds and swarms. Instrumentation on the bug zappers logs the GPS location, altitude, weather details, and time of each mosquito hit. Mosquito control offices can use this information to analyze the insects' activities. The device can be mounted on a remote-controlled or autonomous unmanned vehicle. If autonomous, the vehicle can use the data collected from the electrified net as feedback to improve the effectiveness of the motion plan.

new image of drone and screen

Initial work simulates a large number of mosquitoes within a rectangular area. Each mosquito obeys a biased random walk flight pattern. The flying robot can eliminate any modeled mosquito that intersects its path, detect the time

M. Burbage, A. Nguyen, K. Walker, N. Phung, V. Truong, E. Van Aller, and A. Becker are with the ECE Department at the University of Houston, TX. [atbecker@uh.edu](mailto:atbecker@uh.edu).



Fig. 1. A multi-copter drone carrying a 60 cm square bug-zapping screen. An onboard microcontroller monitors the voltage across the screen and records the time, GPS location, altitude, and weather information for each mosquito strike. Video is available at <https://youtu.be/1gvJ-yTf-E8> [4].

each mosquito is eliminated, and use this data as feedback for a motion policy.

## II. RELATED WORK

### A. Mosquito Control Solutions

Mosquito control has a long history of efforts associated both with monitoring mosquito populations [5] and with eliminating mosquitoes. The work involves both draining potential breeding grounds and destroying living mosquitoes [6]. An array of insecticidal compounds has been used with different application methods, concentrations, and quantities, including both larvicides and compounds directed at adult mosquitoes [7].

Various traps have been designed to capture and/or kill mosquitoes with increasing sophistication in imitating human bait as designers strive to achieve a trap that can rival the attraction of a live human [8]. In recent history, methods have also included genetically modifying mosquitoes so that they either cannot reproduce effectively or cannot transmit diseases successfully [9], and with the recent genomic mapping of mosquito species, new ideas for more targeted work have been formulated [10].

### B. Robotic Pest Management

As GPS technology has flourished and data processing has become cheaper and more readily available, researchers have explored options for implementing the new technologies in

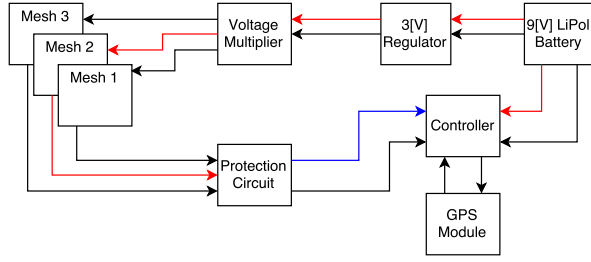


Fig. 2. Block diagram of microcontroller and bug zapper.

breeding ground removal [11] and more effective insecticide dispersion [12]. Low cost drones for residential spraying are under development [13]. Even optical solutions have been considered, including laser containment [14] or, by extension, exclusion and laser tracking and extermination [15].

### C. Robotic coverage

Robotic coverage has a long history. The basic problem is one of designing a path for a robot that ensures the robot visits within  $r$  distance of every point on the workspace. For an overview see [16]. This work has been extended to use multiple coverage robots in a variety of ways, including using simple behaviors for the robots [17], [18]. The key difference in the mosquito coverage problem is that the mosquitoes can move, recontaminating an area previously cleared. We instead have a probability of coverage, as in [19]. This is closely related to the art gallery problem [20] but with limited range of visibility.

## III. DESIGN

This section examines the components of the mosquito drone system, shown in Fig. 1. This includes the electronics, electrified screen, energy budget, UAV, and design parameters. The design for the mosquito drone system been assigned U.S. Provisional Patent Application [21].

### A. Electronics

Fig. 2 shows a block diagram of the control circuit. The system is powered by a 9 V Lithium Polymer battery applied directly to the controller. The 9 V supply is also regulated down to 3 V and applied to the voltage multiplier circuit that powers the mesh of the net, as shown in Fig. 3. One or more meshes may be used to enable localization of mosquito hits. The net output is a high voltage across the screen mesh. A protection circuit steps this voltage down to a suitable level for monitoring by the ADC of the controller. The controller uses a GPS shield for monitoring the location and altitude as well as a real time clock to timestamp each data point collected from the system.

new description of circuit and a new image

A circuit diagram of both the bug zapper and the probe is shown in Fig. 3. The bug zapper (shown on the left) uses a

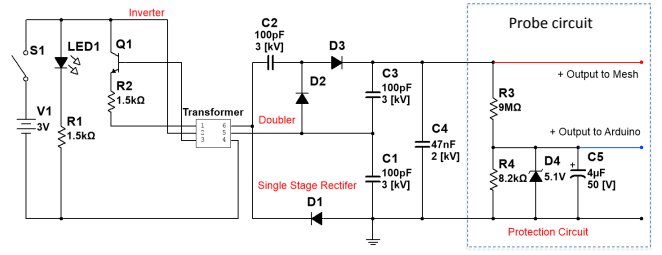


Fig. 3. Circuit diagram of the bug zapper and probe circuit.

BJT (Q1) and center tap transformer to invert a DC input voltage to AC and apply it to the primary winding of a step-up transformer (1:1000). The voltage at the secondary winding of the transformer is boosted and rectified to a high voltage output capacitor that is applied to the inner layer of the mesh. The probe (shown on the right) uses a voltage divider to lower the voltage so that it can be monitored by the microcontroller. A Zener diode (D4) placed in parallel protects the ADC input.

### B. Screen

new description of screen

The screen is constructed with two layers of wire mesh with 3.6 mm openings with a layer of wire mesh with 0.74 mm openings suspended between them. A balsa wood frame insulates the outer meshes from the inner mesh. This mesh arrangement weighs 1633 g/m<sup>2</sup>. The payload that the drone can reliably carry is used to select a size that satisfies the requirements, 60 cm for this multi-coptor drone.

### C. Drone

describe the drone

### D. Energy Budget

what is the new energy usage of the screen?

Tests with an oscilloscope show that in the steady state, a 60 cm × 60 cm screen and electronics have a power consumption of 3.6 W. During a zap, the screen voltage monitoring circuit shorts briefly when the mosquito contacts the screen. Fig. 4 shows the time sequences for battery and screen voltages, current, and power during five mosquito zaps. The initial current spike recovery can be modeled with an exponential fit.

$$i = 69.1e^{-2.7 \times 10^4 t} \text{ A} \quad (1)$$

The fit in (1) gives us a time constant of  $2.7 \times 10^4 / s$  for the short and a recovery time of 80 μs. Multiplying

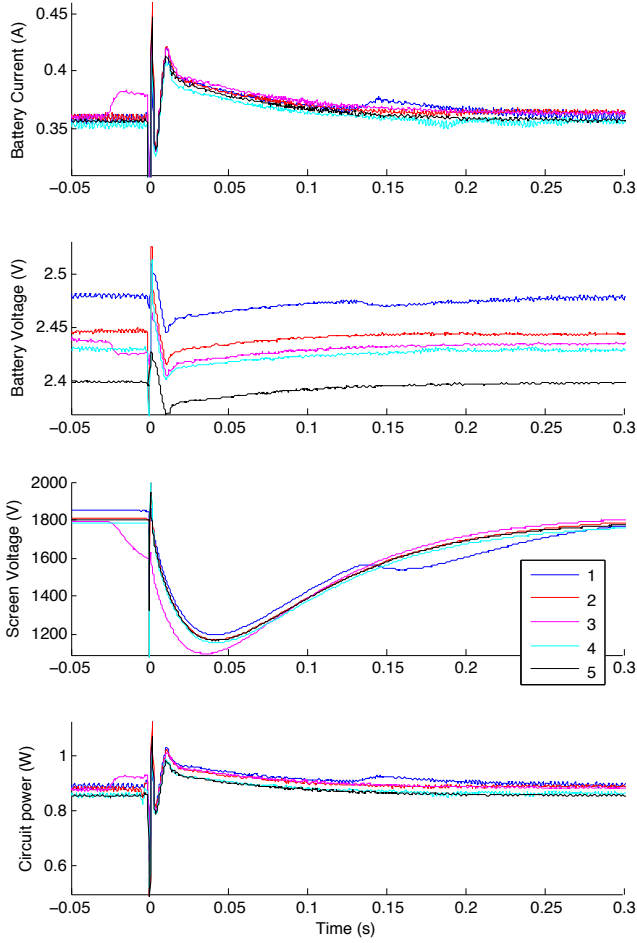


Fig. 4. Current, voltage, and power traces for five *Culex quinquefasciatus* mosquitoes as each contacts the bug-zapping screen. Contact causes a brief short that recovers in 160 ms.

voltage by current to find the instantaneous power ( $p = iv$ ) and integrating the area under the power curve show a total energy consumption of 4.2 mJ for each zap. Recharging the screen requires more power and is represented in the latter part of the curves. The overall recovery time is about 160 ms. Most of the energy is consumed charging and maintaining the charge on the screen rather than in zapping the mosquitoes.

#### E. Location of screen

The drone carries the bug-zapping screen, which is suspended by fishing line at each corner. The location of this screen determines the efficacy of the mosquito drone, measured in mosquitoes eliminated per second of flight time.

For manufacturing ease, the electrified screen is a square measuring  $d_s$  on each side. The mosquito species we are initially targeting fly at low altitude, so the screen is suspended a distance  $h_s$  beneath the drone flying at height  $h_d$ . Suspending this screen beneath the drone improves efficiency because a hanging screen requires less weight than a rigid frame to hold the screen above the drone. This screen can be suspended at any desired angle  $\theta$  in comparison to horizontal, as shown in Fig. 5. A key question is what distance  $h_s$  the screen

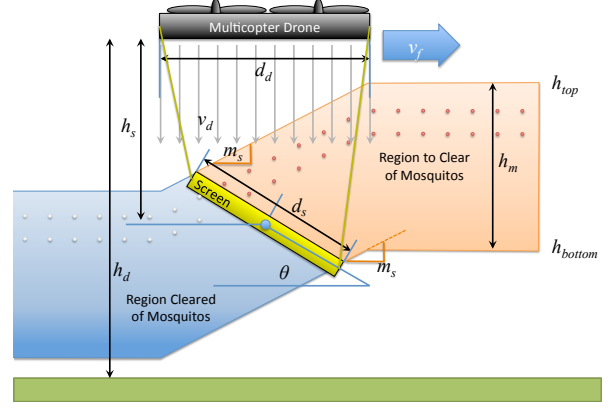


Fig. 5. The drone suspends a square bug-zapping screen beneath it. Propwash pushes incoming mosquitoes downwards, and the drone clears a volume  $h_m \times d_s \times v_f$ . Circles show two mosquitoes at equal time intervals relative to the drone.

should be suspended from the drone, and the optimal angle  $\theta$ . The goal is to clear the greatest volume of mosquitoes per second, a volume defined by the drone forward velocity  $v_f$  and the cross sectional area  $h_m \times d_s$  cleared by the screen, as shown in Fig. 6.

To hover, the drone must push sufficient air down with velocity  $v_d$  to apply a force that cancels the pull of gravity. The drone has mass  $m_d$  and its cross section can be approximated as square-shaped with size  $d_d \times d_d$ . The mass flow of air through the drone's props is equal to the product of the change in velocity of the air, the density of the air  $\rho_a$ , and the cross sectional area.

We assume that air above the drone is quiescent, so the change in velocity of the air is  $v_d$  m/s.

$$\begin{aligned} \text{Force gravity} &= (\text{mass flow}) \cdot \text{air velocity} \\ m_d \cdot g &= (v_d \cdot \rho_a \cdot d_d^2) \cdot v_d \end{aligned} \quad (2)$$

Then the required propwash, the velocity of air beneath the drone, for hovering is

$$v_d = \sqrt{\frac{m_d g}{\rho_a d_d^2}} \quad (3)$$

The drone testing site in Houston, Texas is 15 m above sea level. At sea level the density of air  $\rho_a$  is 1.225 kg/m<sup>3</sup>. The 3DR Solo drone weighs 2 kg with a diameter of 0.71 m [22]. The acceleration due to gravity is 9.871 m/s<sup>2</sup>. Substituting these values into (3) gives  $v_d = 5.6$  m/s.

Due to propwash, an initially hovering mosquito will fall when under the drone at a rate of  $v_d$ . Relative to the drone the mosquito moves horizontally  $-v_f$ . As shown in Fig. 5, we can extend lines with slope  $v_d/v_f$  from the screen's trailing

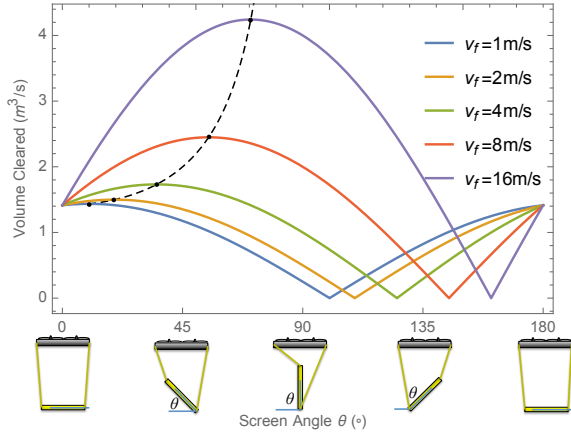


Fig. 6. The volume cleared by a drone is a function of screen angle  $\theta$  and forward velocity  $v_f$ . The dotted line shows the optimal angle given in (5).

edge to  $h_{top}$  and from the leading edge to  $h_{bottom}$

$$h_{top} = h_d - h_s + \frac{d_s}{2} \sin(\theta) + \frac{d_d + d_s \cos(\theta)}{2} \frac{v_d}{v_f}$$

$$h_{bottom} = h_d - h_s - \frac{d_s}{2} \sin(\theta) + \frac{d_d - d_s \cos(\theta)}{2} \frac{v_d}{v_f}$$

$$h_m = h_{top} - h_{bottom} = d_s \left( \frac{v_d}{v_f} \cos(\theta) + \sin(\theta) \right) \quad (4)$$

The optimal angle is therefore a function of forward and propwash velocity:

$$\theta = \text{ArcTan} \left( \frac{v_f}{v_d} \right) \quad (5)$$

To ensure the maximum number of mosquitoes are collected, the screen must be sufficiently far below the drone  $h_s > \frac{d_s}{2} \sin(\theta) + \frac{d_d + d_s \cos(\theta)}{2} \frac{v_d}{v_f}$  and the bottom of the screen must not touch the ground,  $h_d > h_s + \frac{d_s}{2} \sin(\theta)$ .

Changing the flying height  $h_d$  of the drone will target different mosquito populations because mosquitoes are not distributed uniformly vertically. Gillies and Wilkes have demonstrated that different species of mosquitoes prefer to fly at different heights [23].

#### IV. SIMULATION

place code on matlab central, describe the new code

Before launching a fully-instrumented drone, this concept was simulated using MATLAB code. One thousand mosquitoes are randomly placed within a square area one hundred meters on a side. A satellite image of Houston was used as the simulation environment, and each mosquito is programmed to move according to a biased random walk at a speed up to  $0.4 \text{ m/s}$  and with a direction heading biased toward the greenest of the pixels surrounding its current position. This imitates the live mosquitoes' preference for vegetative areas. The simulation is initialized by a mosquito

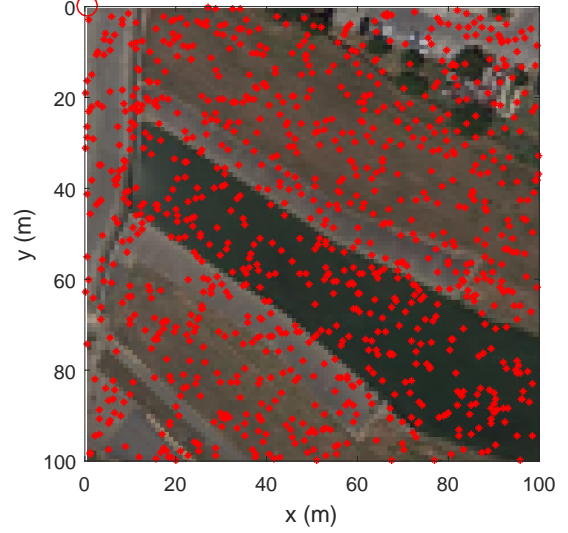


Fig. 7. A  $100 \text{ m} \times 100 \text{ m}$  image with one thousand simulated mosquitoes (red markers). The mosquitoes have had 1.4 hours to bias themselves toward green areas of the image. The robot (red circle) is shown at the upper left corner, preparing to start a bug-zapping run.

distribution generated by running the mosquito movement routine five thousand times, simulating 1.4 hours of flying time, before the robot begins to search (Fig. 7). Because mosquitoes do not care about boundaries, a toroidal mapping is used to keep them in the workspace.

Two different routines handle the robot's path. The first uses a random bounce algorithm. The robot begins in the center of the workspace and moves with a heading that varies randomly up to  $\pm 0.2 \text{ rad}$  from its previous heading and bounces off the perimeter of the workspace with a random heading equally biased between 0 and  $2\pi$ , excluding headings leading outside the workspace. The velocity is set at a prescribed speed.

The second algorithm uses a boustrophedon path [16]. The robot begins in one corner of the workspace and methodically progresses back and forth, advancing one screen width at each turn. If it covers the entire field in the allotted time, it begins covering the field again.

To keep the routines comparable, the robots use the same speed and same number of iterations. These simulations used  $12 \text{ m/s}$  and fifteen minutes of flying time. They also used the same image for biasing the mosquito flight.

For the main body of the simulation, a loop runs a series of iterations in which each mosquito moves one step and the robot moves one step. In that step, the path traced by the bug-zapping screen is calculated, and any mosquitoes in that path are considered to have been killed.

One hundred trials were performed with each coverage path and the results evaluated. The boustrophedon successfully covered the entire field in every trial ( $\mu = 100\%$ ,  $\sigma = 0\%$ ) and covered a portion of the area a second time, while the random bounce covered only 67.9% of the field ( $\mu = 67.9\%$ ,  $\sigma = 1.0\%$ ) with a considerable amount of



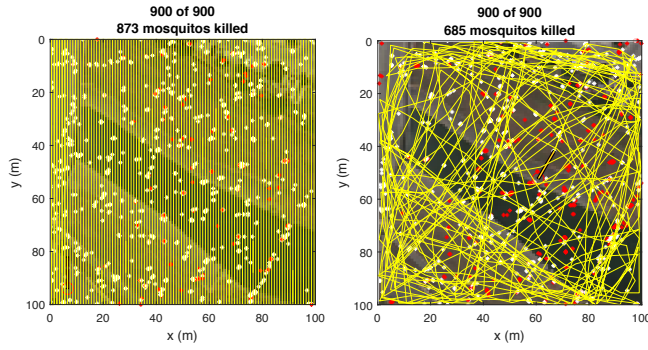


Fig. 8. Boustrophedon robot (left) and random bounce (right) path (yellow lines) overlaid upon a  $100\text{ m} \times 100\text{ m}$  image. The robot (red circle) and the area covered by the bug-zapping net in an iteration (red rectangle) are shown along with a population of a thousand mosquitoes. Those killed during the simulation are white, and those that survived are red.

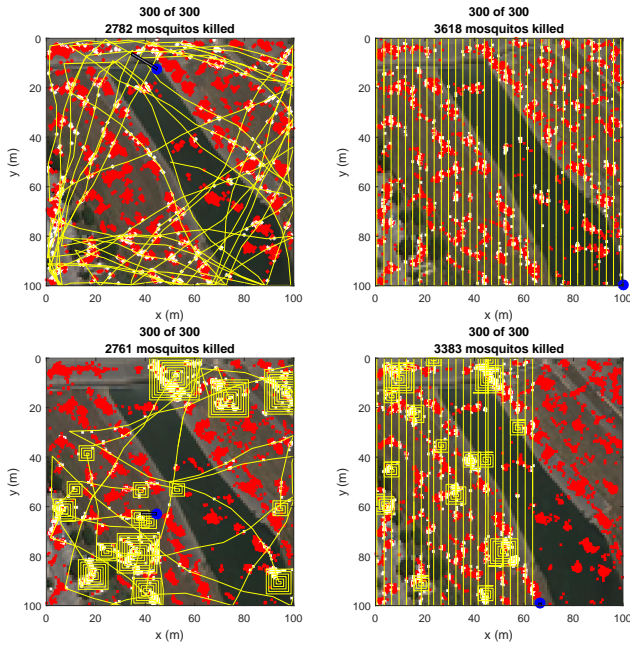


Fig. 9. Left column random bounce, right column boustrophedon. Bottom row adds a subroutine to perform spiral movements when the mosquito density is high.

overlap. As a result, the boustrophedon killed significantly more mosquitoes ( $\mu = 87.7\%$ ,  $\sigma = 1.1\%$ ) than the random bounce ( $\mu = 68.6\%$ ,  $\sigma = 2.7\%$ ). In fact, the smallest number of mosquitoes killed in 100 trials by the boustrophedon (84.1%) was considerably larger than the largest number killed by the random bounce (75.1%). Fig. 9 and Fig. ?? show the paths for boustrophedon and random bounce trials, respectively.

## V. EXPERIMENT

replace with the new experiment description

Before mounting an instrumented screen to a drone, proof of concept experiments used three commercial bug zappers

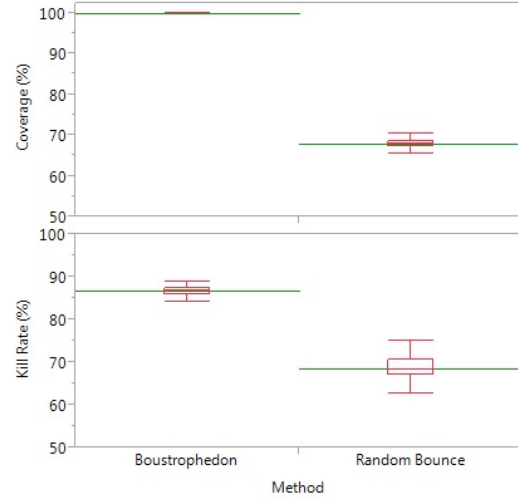


Fig. 10. Comparison of percentage of area covered and percentage of mosquitoes killed for the boustrophedon and random bounce coverage patterns. Plots show aggregate results of 100 trials, using the workspace shown in Fig. 7.

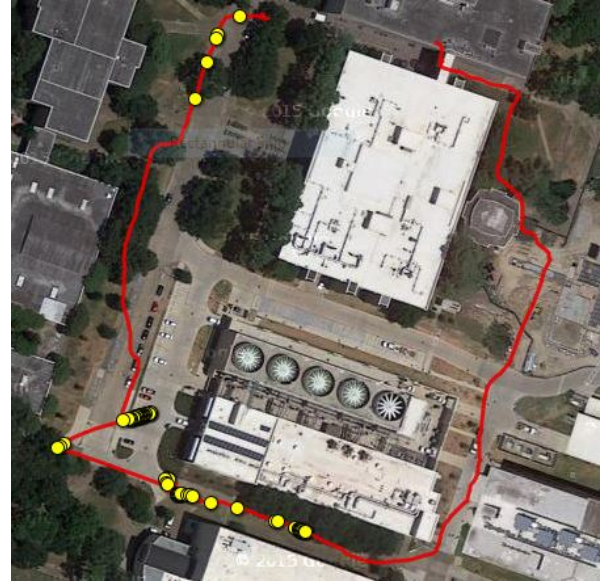


Fig. 11. Satellite image overlaid with GPS path (red line) and kill locations (yellow circles) from proof of concept trial. Visualization using [24].

mounted on a pole with two controllers and a GPS tracker as shown in Fig. ?. The circuits were powered with a  $9\text{ V}$  battery as described above. One controller logged the GPS data at one second intervals while the other continuously tracked the voltage across each bug zapper mesh. Both sets of data are time-stamped so that they can be correlated to determine the location of each kill. Fig. 11 shows the circuit around a pair of buildings followed in an early trial with the kill locations superimposed upon it.

## VI. CONCLUSION AND FUTURE WORK

Initial tests indicate that we can use our instrumentation to track the location of a mosquito-killing drone as it patrols a field and that we can detect and map mosquito kills.

Simulation has shown that covering the field thoroughly leads to a higher success rate when killing mosquitoes. Because the mosquitoes move around, the robot will not kill all the mosquitoes in a single trial as some can fly into a previously covered area as the robot approaches them; however, the chances of killing the mosquitoes increase as the coverage increases.

There are a number of refinements to the simulation algorithm that could be pursued in future work. Refinements are possible in both the mosquito-biasing algorithm and the robot flight simulation. The model may be expanded to three dimensions. Additional search paths may be compared to the existing algorithms. These and other considerations will make a more realistic model for future work. Full instrumentation of the multi-copter drone will allow more extensive testing of the hardware design and will allow field tests of the simulation algorithms.

New sensors are being developed that can identify and detect flying insects, [25]. These sensors may enable a drone to proactively steer toward insect swarms and identify insects in realtime.

#### ACKNOWLEDGMENT

The authors acknowledge the helpful advice and feedback from Martin Reyna Nava, MS, Medical Entomologist and Technical Operations Manager and Mustapha Debboun, Ph.D, BCE, Director Mosquito Control Division, of the Harris County Public Health & Environmental Services, Mosquito Control Division.

This material is based upon work supported by the National Science Foundation under Grant No. IIS-1553063. Any opinions, findings, and conclusions or recommendations expressed in this material are those of the authors and do not necessarily reflect the views of the National Science Foundation.

#### REFERENCES

- [1] C. J. Murray, L. C. Rosenfeld, S. S. Lim, K. G. Andrews, K. J. Foreman, D. Haring, N. Fullman, M. Naghavi, R. Lozano, and A. D. Lopez, "Global malaria mortality between 1980 and 2010: a systematic analysis," *The Lancet*, vol. 379, no. 9814, pp. 413–431, 2012.
- [2] M. O. Ndiath, S. Sougoufara, A. Gaye, C. Mazonot, L. Konate, O. Faye, C. Sokhna, and J.-F. Trape, "Resistance to ddt and pyrethroids and increased kdr mutation frequency in *An. gambiae* after the implementation of permethrin-treated nets in senegal," *PLoS One*, vol. 7, no. 2, p. e31943, 2012.
- [3] sciencedaily.com. (1997, Jul.) Snap! crackle! pop! electric bug zappers are useless for controlling mosquitoes, says uififas pest expert. [Online]. Available: <http://www.sciencedaily.com/releases/1997/07/970730060806.htm>
- [4] A. Nguyen. (2016, Mar.) Uav with instrumented bug zapper. [Online]. Available: <https://youtu.be/1gvJ-yTf-E8>
- [5] J. A. Dennett, A. Bala, T. Wuithiranyagool, Y. Randle, C. B. Sargent, H. Guzman, M. SIIRIN, H. K. Hassan, M. Reyna-Nava, T. R. Unnasch *et al.*, "Associations between two mosquito populations and west nile virus in harris county, texas, 2003–06," *Journal of the American Mosquito Control Association*, vol. 23, no. 3, p. 264, 2007.
- [6] R. Peter, P. Van den Bossche, B. L. Penzhorn, and B. Sharp, "Tick, fly, and mosquito control—lessons from the past, solutions for the future," *Veterinary parasitology*, vol. 132, no. 3, pp. 205–215, 2005.
- [7] W. H. Organization, "Guidelines for laboratory and field testing of mosquito larvicides," *WORLD HEALTH ORGANIZATION COMMUNICABLE DISEASE CONTROL, PREVENTION AND ERADICATION WHO PESTICIDE EVALUATION SCHEME*, 2005.
- [8] D. V. Maliti, N. J. Govella, G. F. Killeen, N. Mirzai, P. C. Johnson, K. Kreppel, and H. M. Ferguson, "Development and evaluation of mosquito-electrocuting traps as alternatives to the human landing catch technique for sampling host-seeking malaria vectors," *Malaria journal*, vol. 14, no. 1, p. 1, 2015.
- [9] J. M. Marshall and C. E. Taylor, "Malaria control with transgenic mosquitoes," *PLoS Med*, vol. 6, no. 2, p. e1000020, 2009.
- [10] C. A. Hill, F. C. Kafatos, S. K. Stansfield, and F. H. Collins, "Arthropod-borne diseases: vector control in the genomics era," *Nature Reviews Microbiology*, vol. 3, no. 3, pp. 262–268, 2005.
- [11] P. Anupa Elizabeth, M. Saravana Mohan, P. Philip Samuel, S. Pandian, and B. Tyagi, "Identification and eradication of mosquito breeding sites using wireless networking and electromechanical technologies," in *Recent Trends in Information Technology (ICRTIT), 2014 International Conference on*. IEEE, 2014, pp. 1–6.
- [12] B. Hur and W. Eisenstadt, "Low-power wireless climate monitoring system with rfid security access feature for mosquito and pathogen research," in *Mobile and Secure Services (MOBISERVICES), 2015 First Conference on*. IEEE, 2015, pp. 1–5.
- [13] J.-T. Amenyio, D. Phelps, O. Oladipo, F. Sewovoe-Ekuoe, S. Jadoonanan, S. Jadoonanan, T. Tabassum, S. Gnabode, T. D. Sherpa, M. Falzone *et al.*, "Medizdroids project: Ultra-low cost, low-altitude, affordable and sustainable uav multicopter drones for mosquito vector control in malaria disease management," in *Global Humanitarian Technology Conference (GHTC), 2014 IEEE*. IEEE, 2014, pp. 590–596.
- [14] C. Boonsri, S. Sumriddetchkajorn, and P. Buranasiri, "Laser-based mosquito repelling module," in *Photonics Global Conference (PGC), 2012*. IEEE, 2012, pp. 1–4.
- [15] J. Kare and J. Buffum, "Build your own photonic fence to zap mosquitoes midflight [backwards star wars]," *IEEE Spectrum*, vol. 5, no. 47, pp. 28–33, 2010. [Online]. Available: <http://spectrum.ieee.org/consumer-electronics/gadgets/backyard-star-wars>
- [16] H. Choset, "Coverage for robotics - a survey of recent results," *Annals of Mathematics and Artificial Intelligence*, vol. 31, no. 1-4, pp. 113–126, October 2001.
- [17] D. Spears, W. Kerr, and W. Spears, "Physics-based robot swarms for coverage problems," *The international journal of intelligent control and systems*, vol. 11, no. 3, 2006.
- [18] S. Koenig, B. Szymanski, and Y. Liu, "Efficient and inefficient ant coverage methods," *Annals of Mathematics and Artificial Intelligence*, vol. 31, no. 1, pp. 41–76, Oct. 2001.
- [19] C. Das, A. Becker, and T. Bretl, "Probably approximately correct coverage for robots with uncertainty," in *IEEE/RSJ International Conference on Intelligent Robots and Systems (IROS)*, vol. 1, San Francisco, CA, USA, Oct. 2011, pp. 1160–1166.
- [20] D.-T. Lee and A. K. Lin, "Computational complexity of art gallery problems," *Information Theory, IEEE Transactions on*, vol. 32, no. 2, pp. 276–282, 1986.
- [21] A. T. Becker, "Unmanned mosquito elimination vehicles," US Patent 62/324,625, 04 19, 2016.
- [22] R. Sollenberger, "Solo specs: Just the facts," May 2015. [Online]. Available: <https://3dr.com/solo-gopro-drone-specs/>
- [23] M. Gillies and T. Wilkes, "The vertical distribution of some West African mosquitoes (Diptera, Culicidae) over open farmland in a freshwater area of The Gambia," *Bulletin of entomological research*, vol. 66, no. 01, pp. 5–15, 1976.
- [24] A. Schneider, "Gps visualizer," Mar. 2003. [Online]. Available: <http://www.gpsvisualizer.com>
- [25] Y. Chen, A. Why, G. Batista, A. Mafra-Neto, and E. Keogh, "Flying insect classification with inexpensive sensors," *Journal of insect behavior*, vol. 27, no. 5, pp. 657–677, 2014.